

Low Carbon Scheduling in Manufacturing Workshops Taking into Account the Improvement of NSGA-II

Yanjun Zhou

Department of Party Committee Teachers' Affairs and Human Resources, Jiaxing Nanyang Polytechnic Institute, China
zhouyanjunzyj@outlook.com

Fei Wang

College of Control Science and Engineering, China University of Petroleum (East China), China
wangfeiff1988@outlook.com

Abstract: *With the increasingly fierce global competition, the manufacturing industry also needs to implement low-carbon scheduling to improve its competitiveness. To achieve the low-carbon goals of manufacturing enterprises, this study first constructs a multi-objective workshop low-carbon scheduling model for manufacturing enterprises. Then, the crossover operator, mutation operator, and elite retention strategy of the Non-Dominated Sorting Genetic Algorithm II (NSGA-II) are improved, which is applied to handle the low-carbon scheduling model between vehicles. When the targets were 20, the proposed model solved two multi-objective optimization test functions with inverse generation distance values of 0.338 and 1.153, and spatial evaluation values of 0.013 and 0.415. The proposed model had a faster solving speed and converged to the optimal solution in about 10 iterations. The proposed model performed the best in solving Low-Carbon Scheduling in Manufacturing Workshops (LSCW), with the shortest maximum completion time of 6.12 hours, the lowest total energy consumption of 6.71×10^5 kJ, and still the lowest carbon emissions of 5.92×10^4 kW/h. The proposed model in solving the low-carbon scheduling model of manufacturing workshops can help reduce carbon emissions in manufacturing workshops and promote the green transformation of the manufacturing industry.*

Keywords: *Workshop low-carbon scheduling, NSGA-II, manufacturing industry, multi-objective optimization, elite retention strategy.*

Received March 11, 2025; accepted September 10, 2025
<https://doi.org/10.34028/iajит/23/1/6>

1. Introduction

Nowadays, reducing Carbon Emissions (CEs) has become an important goal for governments and businesses around the world. CE is one of the key influencing factors for the continuous deterioration of the environment and the intensification of haze, and classical Manufacturing Industry (MI) often suffer from problems such as energy waste, low efficiency, and high CE [9]. How to reduce CE and improve energy efficiency in MI is a key issue. As the core link of MI, the production workshop has high Energy Consumption (ES) and serious CE problems. Low Carbon Scheduling in MI Workshop (MI-LSCW) is of great significance for reducing Manufacturing Industry Carbon Burden (MICB) [10]. Low Carbon Scheduling in the Workshop (LSCW) helps achieve the sustainable development goals of enterprises by optimizing production processes and resource utilization [28]. However, as the complexity of MI systems increases and the flexible resources increases, the complexity and difficulty of LSCW also sharply increase, requiring enterprises to research more efficient scheduling strategies to cope with increasingly complex manufacturing environments [25]. The Non dominated Sorting Genetic Algorithm

II(NSGA-II) is introduced in workshop scheduling. It is used in workshop scheduling problems to simultaneously optimize multiple objective functions, aiming to optimize job completion time, reduce CE, and balance machine load, thereby improving production efficiency and reducing environmental impact [29]. However, currently NSGA-II still has insufficient convergence and local convergence issues in LSCW, which limits its performance in solving LSCW problems. Thus, this study builds a Multi-Objective (MO) MI-LSCW model and uses Improved NSGA-II (INSGA-II) to calculate the LSCW model. This study aims to provide effective LSCW for MI. The innovation of this study lies in proposing an improved Elite Retention Strategy (ERS) to address the issue of poor diversity in NSGA-II, which can determine the number of elites to be retained with a certain proportion to avoid the loss of population diversity. The following is a summary of the content of this study:

- 1) The current research status is analyzed.
- 2) Multi-objective MI-LSCW has been built and NSGA-II has been improved.
- 3) The proposed model is subjected to application effect analysis.

4) The entire study has been summarized.

2. Related Work

LSCW aims to reduce ES and CE in the workshop production process through reasonable scheduling arrangements, thereby achieving the goals of efficient manufacturing and energy conservation and emission reduction. Li *et al.* [8] constructed a novel model that included real-time task list updates and non-periodic departure methods, and validated it through practical cases. The proposed dynamic scheduling model could reassign automatic guided vehicles, and had certain feasibility and effectiveness. Yang *et al.* [26] built a MO production scheduling offloading optimization model, and solved the model using intelligent algorithms. The method effectively balanced production efficiency and computational latency. Ning and Huang [15] developed a mathematical model to minimize completion time, workload, and CE. They also proposed an enhanced model with double-chain encoding that could meet the MI workshop's emission reduction requirements during production and processing. Xu *et al.* [24] introduced a switching strategy during the idle time of equipment in the MI workshop to establish a model, and used intelligent algorithms to calculate the model, which had certain effectiveness. Mou *et al.* [14] established a fuzzy programming model, and proposed a machine learning based multi strategy approach to solve the model. The proposed method could effectively solve the reverse workshop scheduling problem. Tliba *et al.* [22] examined the dynamic scheduling problem in a real mixed-flow workshop. They established a simulated 3D workshop model and proposed a dynamic scheduling model with digital twins. This model demonstrated promising application results in the 3D workshop. Shao *et al.* [17] built a MO meme algorithm using, and utilized a decoding strategy to decline the search space of subproblems. They obtained all the metrics in the comparison algorithms within a limited running time.

NSGA-II simplifies the complexity associated with non-dominated sorting, offering advantages such as rapid execution speed and effective convergence. Feng *et al.* [3] established a multi-level cross planning matrix and proposed an overall layout planning model for landscape ceramic sculptures with NSGA-II. The optimal layout optimization rate could reach over 60%, which could effectively improve the layout planning of sculptures. Zhang [27] improved the NSGA-II and proposed an MO optimization model with lower iteration curves in cost, time, and environmental objective functions than classical NSGA-II, demonstrating better MO optimization performance. To further promote the widespread application of NSGA-II, Ma *et al.* [11] conducted a comprehensive investigation of its related research work, classified its applications in the engineering field, and discussed its future research potential. Ma *et al.* [12] built a meta

model for welding quality indicators through orthogonal experiments and proposed a MO optimization model for welding process parameters with NSGA-II. The optimized welding process parameters could increase the depth of sidewall fusion and helped improve the overall quality of ultra-narrow gap welding processes. Kabiri *et al.* [5] proposed a three-level dual objective programming model, and solved it using NSGA-II. This method could achieve maximum profit and minimize greenhouse gas emissions. Zhuo *et al.* [31] built a surrogate model for the relationship between process parameters and quality evaluation indicators based on Gaussian process regression, and achieved MO optimization using NSGA-II. It has good prediction performance and stability, with relatively small relative error values. Tang *et al.* [20] constructed a MO optimization model for path planning, and proposed an optimized NSGA-II. The waiting time of the proposed method was reduced by 42.39%, and the no-load distance was reduced by 10.50%.

In summary, although many researchers have analyzed the workshop scheduling problem and proved the application effect of NSGA-II in solving optimization scheduling problems, NSGA-II still has insufficient convergence and local convergence problems. To this end, this study proposes an INSGA-II, aiming to achieve faster low-carbon scheduling in workshops and create greater environmental benefits for businesses and society.

3. LSCW Solution with INSGA-II

To effectively reduce CE in the MI workshop, this study will construct an MI-LSCW model that integrates completion time, total ES, and CE. Subsequently, improvements were made to the crossover operator, mutation operator, and ERS of NSGA-II, and INSGA-II is applied.

3.1. MI-LSCW Model Construction

To effectively reduce CE in the MI workshop, this study conducts MI-LSCW mathematical modeling. LSCW is an optimization model that involves multiple production processes and equipment, with the aim of specifying the machining sequence for different workpieces and achieving optimal resource allocation for workshop scheduling production [1]. n workpieces are processed by m different machine tools, and each workpiece undergoes multiple different processes in a certain order. Figure 1 shows the workpiece processing process in the MI workshop.

To meet the needs of actual production, this study selected three optimization objectives when constructing MI-LSCW: minimizing the Maximum Completion Time (MCT), the total ES of the workshop, and the total amount of CE. The objective function f_1 for minimizing the MCT is shown in Equation (1).

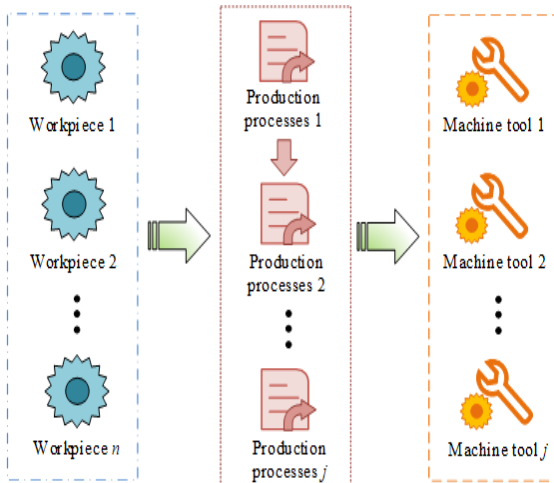


Figure 1. The workpiece processing process.

$$\left\{ \begin{array}{l} f_1 = \min(\max(T_i)) \\ T_i = \sum_{j=1}^{p_i} \sum_{k=1}^m (T_{ijk}^{ob} + T_{ijk,h}^k) \cdot X_{ijk} \end{array} \right. \quad (1)$$

In Equation (1), T_i is the completion time of workpiece i . p_i represents the quantity of processes of workpiece i . T_{ijk}^{ob} is the processing time of the j^{th} process of workpiece i on machine tool k . X_{ijk} represents the transportation time from machine tool h to k . X_{ijk} is the decision variable. When its value is 1, the j^{th} process of workpiece i is processed on machine tool k . Otherwise, its value is 0. The objective function f_2 is shown in Equation (2).

$$f_2 = \sum_{k=1}^m \left[\left(\sum_{i=1}^n \sum_{j=1}^{p_i} T_{ijk}^{ob} X_{ijk} \right) E_c + (T_k - T_k^o - T_{ijk}^{ob} X_{ijk}) E_u \right] + (\max(T_i)) E_i \quad (2)$$

In Equation (2), E_c denotes the ES per unit time during the machining process of machine tool k . T_k denotes the completion time of machine tool k . T_k^o denotes the start-up time of machine tool k . E_u denotes the ES per unit time when machine tool k is idling. E_i is the ES per unit time in the workshop. In Figure 2, this study divides the main sources of CE in the MI workshop into the basic CE generated by machine tool operation and the CE generated by other auxiliary transportation equipment.

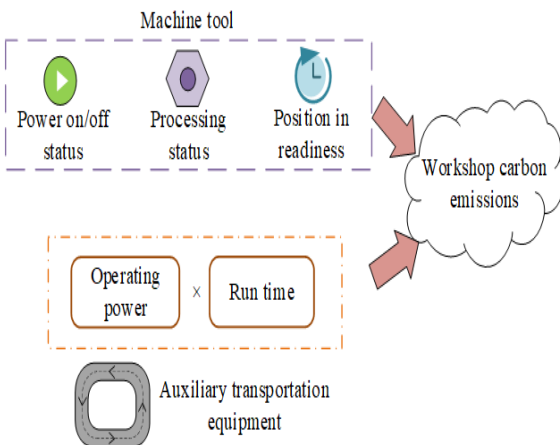


Figure 2. The main source of CE in manufacturing workshops.

In Figure 2, the main CE of the MI workshop is concerned with the operating status of the machine tools, the operating power and time of the auxiliary transportation equipment. The operating status of the machine tool includes on/off state, processing state, and standby state. The on/off state of a machine tool refers to the ES generated by the machine tool from the off state to the on state, as well as from the on state to the off state. The calculation of CE Q^{oc} during this process is shown in Equation (3).

$$Q^{oc} = \sum_{k=1}^m (P_k^o \cdot T_k^o + P_k^c \cdot T_k) \times \xi \quad (3)$$

In Equation (3), P_k^o and P_k^c represent the starting power and unloading power of machine tool k , respectively, in kW. ξ represents the electrical energy CE conversion factor. The calculation of CE Q^{ob} for machine tool machining is shown in Equation (4).

$$Q^{ob} = \sum_{i=1}^n \sum_{j=1}^{p_i} \sum_{k=1}^m P_k^{ob} T_{ijk}^{ob} \xi \times X_{ijk} \quad (4)$$

In Equation (4), P_k^{ob} is the machining power of the machine tool k , in kW. Standby CE is the CE generated when the machine tool is in standby mode, during which the machine tool is not fully utilized. Therefore, standby CE can be reduced by shutting down and restarting or arranging the processing sequence reasonably. To determine whether a shutdown and restart strategy is needed for the machine tool, the difference in time and CE between the machine tool's standby state and the shutdown and restart strategy needs to be considered. Figure 3 is a schematic diagram of determining whether to shut down and restart the strategy.

This study assumes that the total number of machining processes of machine tool k is, and the calculation of machine tool standby CE Q^{pre} considering shutdown and restart operations is shown in Equation (5).

$$Q^{pre} = \sum_{k=1}^m \sum_{t=1}^{B_k} \left((S_{k(t+1)} - U_{kt}) \times P_k^{pre} \times (1 - Z_{kt}) + Z_{kt} E_k^{off} \right) \times \xi \quad (5)$$

In Equation (5), $S_{k(t+1)}$ is the starting processing time of the $t+1^{th}$ process of machine tool k . U_{kt} represents the end processing time of the t^{th} process of machine tool k . E_k^{off} is the standby power of the machine tool k , in kW. Z_{kt} is the decision variable, when its value is 1, the shutdown and restart strategy is executed. E_k^{off} represents the ES required for one shutdown and restart strategy. The calculation of CE for auxiliary equipment Q^a is shown in Equation (6).

$$Q^a = \sum_{i=1}^n \sum_{j=1}^{p_i} P^a T_{ij,h}^k \times \xi \quad (6)$$

In Equation (6), P^a is the power of the auxiliary

equipment, in kW. Therefore, the objective function f_3 of minimizing the total CE is shown in Equation (7).

$$f_3 = \min Q_{total} = \min(Q^{oc} + Q^{ob} + Q^{pre} + Q^a) \quad (7)$$

In Equation (7), Q_{total} represents the total amount of CE. In addition, to improve the quality and practicality of the scheduling scheme, the MI-LSCW model also needs to satisfy the following five constraints. First, the same workpiece and process can only be processed by one machine tool. Secondly, interruptions are not allowed during the machining process of the workpiece. Thirdly, the first process of each workpiece does not take into account transportation time. Fourth, there is a sequential order between different processes of the same workpiece, and only after the current process is completed can the next process be entered. Fifth, the completion time of each workpiece shall not exceed the MCT.

3.2. Solution of LSCW with INSGA-II

The MI-LSCW requires finding a balance point between multiple objectives. Therefore, this study applies NSGA-II to calculate the model. In MO problems, there is a Pareto front composed of a set of solutions [2, 21]. Figure 4 shows the NSGA-II's process.

In Figure 4, NSGA-II introduces strategies such as fast non-dominated sorting, crowded distance, and elite retention, making it efficient and high-precision in MO optimization problems. Non-dominated solution refers to a B_k solution that is superior to other solutions in at

least one objective, while not inferior to other solutions in other objectives. It improves any objective function without weakening the performance of other objective functions. Fast non-dominated sorting is a non-dominated solution search algorithm used for MO optimization problems, which divides the solution set into multiple non-dominated layers, where the solutions in each layer do not dominate each other, but the solutions within each layer dominate the solutions in other layers, thus finding the Pareto optimal solution set with less computational cost [7]. First, the quantity of individuals n_p that dominate individual p in the population and the dominating solution set S_p of individual p are calculated. Secondly, if there is an individual $n_p=0$, it is placed in the first layer and saved in the set F_1 . Then, the dominance correlation between the individual in F_1 and other individuals is compared, and the dominance solution set is updated. Subsequently, for each individual in F_1 , n_p is subtracted by 1. If $n_p=0$ is satisfied after subtracting 1, the individual is placed in the second layer and saved in the set F_2 . This operation is repeated until all individuals are stratified. Finally, all stratified individuals are saved to the corresponding result set. Crowding distance is an indicator used to evaluate solutions to MO problems, which evaluates the crowding distance of individuals by calculating the density around them, helping to avoid the population falling into local optima [16, 23]. Taking the two objective minimization problem as an example, Figure 5 presents the schematic diagram of crowding distance.

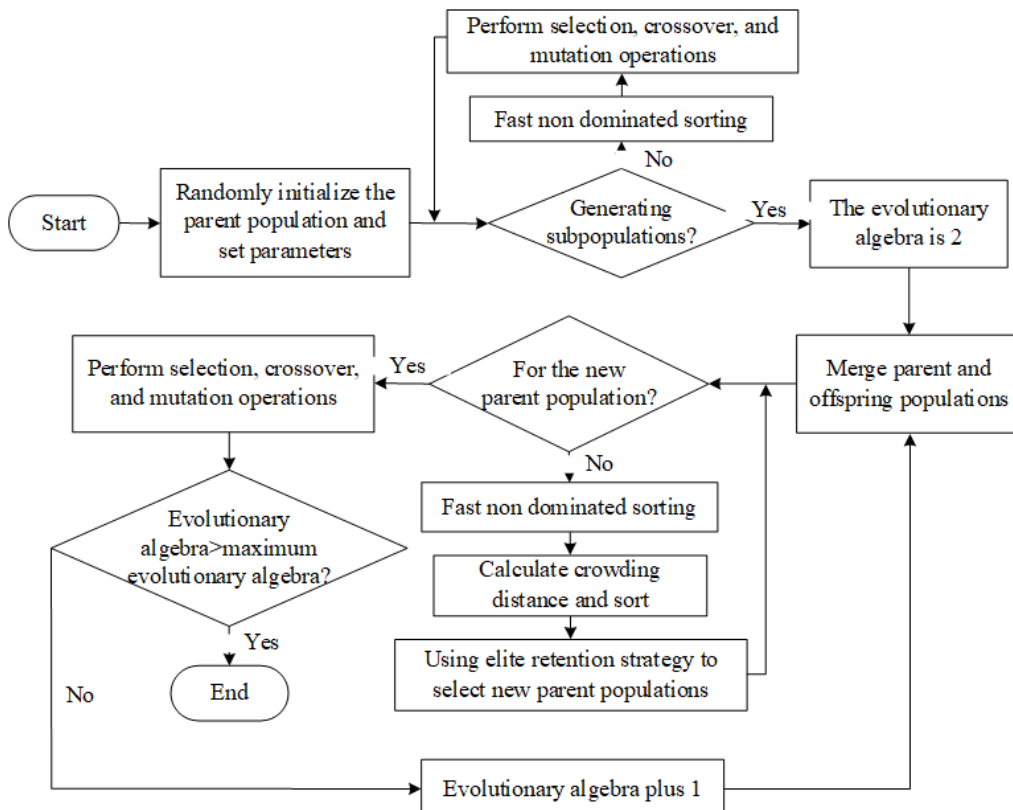


Figure 4. The flowchart of NSGA-II.

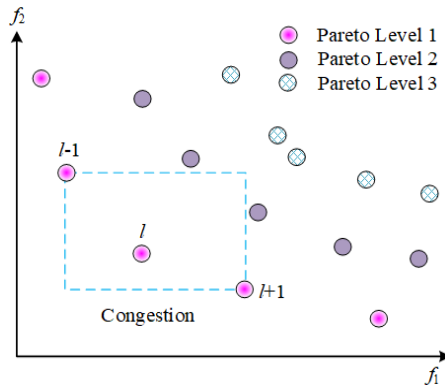


Figure 5. Schematic diagram of crowded distance.

Crowding distance can measure the distribution uniformity and diversity among individuals in a population, to avoid the algorithm getting stuck in local optima. The calculation of crowding distance d_i usually involves hierarchical storage of all individuals in the population, see Equation (8).

$$d_i = \sum_{o=1}^a (|f_o^{l+1} - f_o^{l-1}|), o = 1, 2, \dots, a \quad (8)$$

In Equation (8), a is the quantity of objective functions. f_o^{l+1} is the function value of individual $l+1$ on the o^{th} objective. f_o^{l-1} is the function value of individual $l-1$. The ERS preserves excellent individuals, enabling the offspring population to inherit superior genetic information during the evolutionary process. This accelerates the convergence speed and optimization effect of the algorithm [19, 30]. Figure 6 shows the ERS.

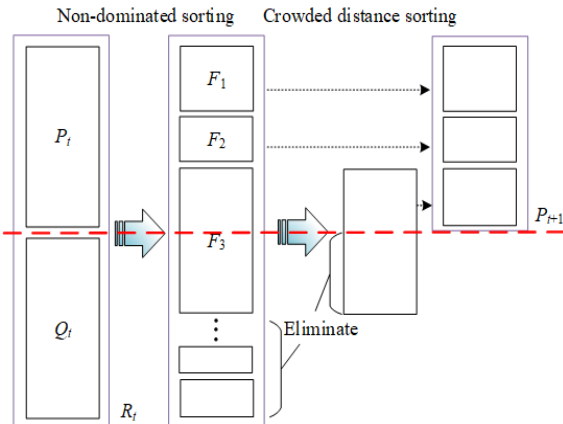


Figure 6. Schematic diagram of ERS.

In Figure 6, the ERS directly replicates specific individuals from the previous generation to the next generation, which can avoid the optimal individual being destroyed due to hybridization operations. Nevertheless, the NSGA-II algorithm has certain limitations; it is susceptible to premature convergence (local optima) and exhibits low convergence efficiency [13]. Therefore, this study proposes an INSGA-II. First, in response to the issue of NSGA-II's inability to ensure that individuals in the population search within nearby regions when generating offspring, this study proposes to determine which operation to perform on individuals

with non-dominated sorting levels and generated random numbers. If the non-dominated sorting level is 1 and the generated random number is less than 0.5, perform a variable neighborhood search operation. If the sorting level is not 1 and the generated random number is greater than or equal to 0.5, selection, crossover, and mutation operations will be performed. Secondly, the crossover and mutation operators of NSGA-II have been improved. NSGA-II simulates the genetic and mutation processes in biological evolution [4, 18]. The crossover probability of the improved crossover operator P_c is calculated as shown in Equation (9).

$$P_c = \begin{cases} P_{cmin} + \frac{P_{cmax} - P_{cmin}}{f_{max} - f_{avg}} (f' - f_{avg}), & f' \geq f_{avg} \\ P_{cmax}, & f' < f_{avg} \end{cases} \quad (9)$$

In Equation (9), P_{cmax} and P_{cmin} represent the largest and smallest values of crossover probability, taken as 0.9 and 0.7. f_{max} and f_{avg} are the largest and average values of fitness. f' represents the larger fitness value between two individuals. After obtaining the maximum value of the parent gene locus, the integers on n gene locus are discretized into j new parent individuals, as shown in Equation (10).

$$e_i^j = x_{i-min} + \frac{(b+1)(x_{i-max} - x_{i-min})}{j-1}, \quad (10)$$

$b = 1, 2, \dots, j; i = 1, 2, \dots, n$

In Equation (10), x_{i-max} and x_{i-min} represent the largest and smallest values on the i^{th} gene locus of the parent chromosome, respectively. Two individuals are selected from the original and new parent individuals, and the starting and ending positions are randomly selected. The genes at this position are partially matched and crossed. The mutation operation introduces new genetic variations by randomly changing some genes of the individual [6]. The mutation probability of the improved mutation operator P_v is shown in Equation (11).

$$P_v = \begin{cases} P_{vmin} + \frac{P_{vmax} - P_{vmin}}{f_{max} - f_{avg}} (f_{max} - f), & f' \geq f_{avg} \\ P_{vmax}, & f' < f_{avg} \end{cases} \quad (11)$$

In Equation (11), P_{vmax} and P_{vmin} represent the largest and smallest values of crossover probability, taken as 0.1 and 0.001, respectively. f represents the fitness value of the mutant individual. The mutant gene x'_m is shown in Equation (12).

$$x'_m = x_m \left[1 + C(0,1) \left(1 - \frac{t}{T} \right) \right] \quad (12)$$

In Equation (12), x_m represents the gene before mutation. $C(0,1)$ represents the Cauchy distribution. t is the current iteration count. T is the largest iteration count. The improved mutation operator has a strong mutation effect, and the degree of mutation gradually decreases gradually, enabling the algorithm to search for more feasible solutions. In addition, this study builds an ERS with population balance to address the issue of reduced species diversity in NSGA-II. Assuming the

population size is N , if the total number of individuals is bigger than N , the top N optimal individual based on crowding distance is retained. If it is equal to N , all individuals in the first non-dominated layer are retained. If the total number of individuals is less than N , the selection of individuals in the x^{th} layer and the calculation of the new population p_{t+1} are shown in Equation (13).

$$\left\{ \begin{array}{l} n_x = \frac{m_x^2}{2N} \\ p_{t+1} = m_1 + \sum_{i=2}^r \frac{m_i^2}{2N}, r = 1, 2, \dots, x \end{array} \right. \quad (13)$$

In Equation (13), n_x represents the quantity of individuals to be selected in the x^{th} layer. m_x is the total quantity of individuals in the x^{th} layer. m_1 represents all individuals in the first non-dominated layer. Figure 7 is a schematic diagram of an improved ERS.

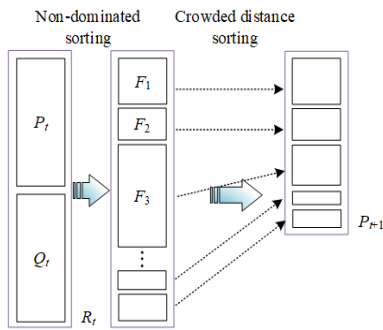
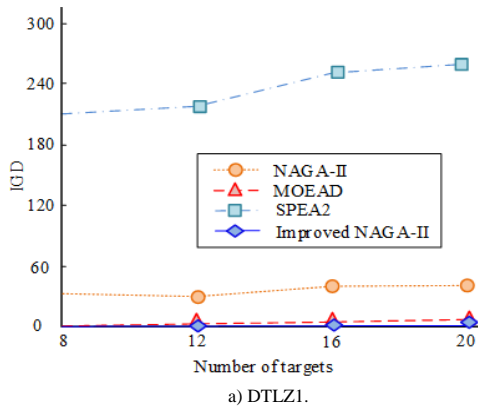


Figure 7. Schematic diagram of improved ERS.

In Figure 7, the proposed improved ERS first retains all individuals in the first non-dominated layer of the population to the new population, and then retains individuals in a certain proportion, which can improve its efficiency.



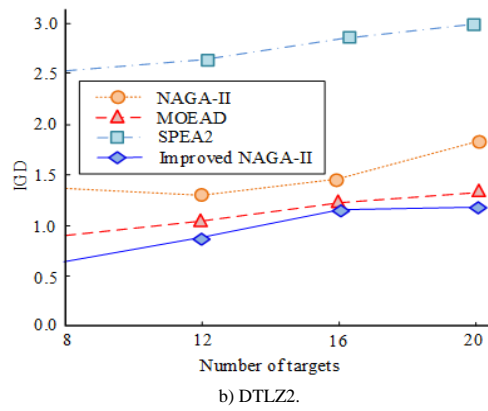
a) DTLZ1.

4. Analysis of Low-Carbon Scheduling Effect with INSGA-II

To validate the performance of the low-carbon scheduling model solving method with INSGA-II, this study applied MO optimization test functions and explored their application effects in solving the MILSCW model through test cases.

4.1. Performance Analysis of INSGA-II

This study used the MO optimization test function Deb Thiele Laumanns Zitzler (DTLZ) for testing. MatlabR2020 was used for simulation experiments, with a computer system of Windows 11, a central processing unit of i7-9800X, and 16GB of memory. The population size was 150 and the largest iterations were 200. INSGA-II was compared with Inverse Generation Distance (IGD), classical NSGA-II, Strength Pareto Evolutionary Algorithm 2 (SPEA2), and Multi-Objective Evolutionary Algorithm with Decomposition (MOEAD). In Figure 8, each algorithm ran independently 30 times. In Figure 8-a), in the solution of DTLZ1, as the number of targets increased, the IGD values of all four algorithms gradually increased. Among them, the IGD value of INSGA-II was always the lowest, and when the target quantity was 20, the IGD value was 0.338. Secondly, MOEAD and SPEA2 had the highest IGD values. In Figure 8-b), INSGA-II still performed the best in terms of IGD metrics in the solution of DTLZ2. When the target quantity was 20, the IGD value was 1.153. INSGA-II achieved good results in IGD indicators, with good convergence and distribution performance.



b) DTLZ2.

Figure 8. Comparison of inverted generation distance among four algorithms.

Figure 9 compares the Spatial Metric (SM) values of the four algorithms mentioned above. In Figure 9-a), as the number of targets increased, the SM values of all four algorithms gradually increased. Among them, INSGA-II performed the best in the SM indicator, with an SM value of 0.013 when the target quantity was 20. In Figure 9-b), the SM value of INSGA-II was still

lower than the other three algorithms, and when the number of targets was 20, the SM value was 0.415. Secondly, MOEAD and classical NSGA-II had the highest SM values. As a result, INSGA-II achieved good results in the SM index, and the algorithm had good convergence.

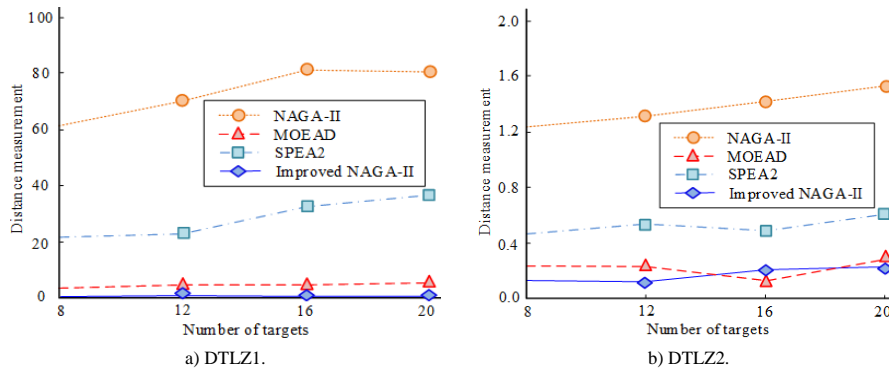


Figure 9. Comparison of spacing metrics for four algorithms.

This study conducted ablation experiments. The target quantity was 8, and INSGA-II was compared with classical NSGA-II, INSGA-II without improved crossover operator (A), INSGA-II without improved mutation operator (B), and INSGA-II without improved ERS (C). All algorithms were independently run 30 times, and the experimental results were presented in the form of mean±standard deviation. Independent sample t-test ($\alpha=0.05$, Bonferroni correction) was used to verify the significant differences between the proposed

improved NSGA-II algorithm and other algorithms. As shown in Table 1, INSGA-II had the best performance in solving DTLZ1 and DTLZ2. It had the lowest IGD and SM values, which were significantly lower than those of algorithms A, B, and C ($p<0.05$) and extremely significantly lower than those of the traditional NSGA-II algorithm ($p<0.01$). Consequently, the enhancement strategy had the potential to significantly enhance the convergence performance of NSGA-II, and had certain feasibility and effectiveness.

Table 1. Results of ablation experiment.

Algorithm	DTLZ1		DTLZ2	
	IGD	SM	IGD	SM
NSGA-II	$34.155 \pm 3.244^{**}$	$54.317 \pm 2.371^{**}$	$1.229 \pm 1.887^{**}$	$0.812 \pm 0.106^{**}$
A	$2.423 \pm 0.239^*$	$0.374 \pm 0.035^*$	$0.639 \pm 0.065^*$	$0.593 \pm 0.052^*$
B	$2.437 \pm 0.242^*$	$0.381 \pm 0.037^*$	$0.647 \pm 0.071^*$	$0.610 \pm 0.057^*$
C	$4.263 \pm 0.433^*$	$0.538 \pm 0.056^*$	$0.865 \pm 0.094^*$	$0.764 \pm 0.069^*$
INSGA-II	$0.230 \pm 0.022^*$	$0.007 \pm 0.001^*$	$0.517 \pm 0.050^*$	$0.329 \pm 0.028^*$

Note: ** indicates a highly significant difference compared to INSGA-II, $p<0.01$, * indicates a significant difference compared to INSGA-II, $p<0.05$.

In Figure 10, the IGD values of the five algorithms mentioned above were compared under different target quantities. In Figure 10-a), as the number of targets increased, the IGD values of different algorithms showed an upward trend. Among them, the IGD value of algorithm C was only inferior to classical NSGA-II, indicating that the improved ERS had a more significant

optimization effect on the algorithm. In Figure 10-b), INSGA-II still performed the best in terms of IGD indicators. Therefore, the improvement strategy had the potential to significantly enhance the performance of NSGA-II, with the contribution of improving the ERS being the greatest.

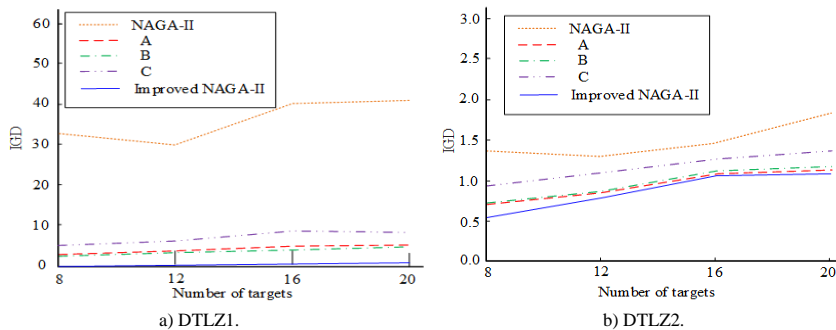


Figure 10. Comparison of IGD values for five algorithms.

4.2. Effect Analysis of MI-LSCW

To test the performance of INSGA-II in handling LSCW model, this study used classic examples such as Kacem and Brandimarte for testing. In Figure 11, the search processes of INSGA-II and classical NSGA-II for solving Kacem01 and Kacem03 problems were compared. In Figure 11-a), both INSGA-II and classical

NSGA-II could solve for the optimal solution, but INSGA-II had a faster solving speed and converged to the optimal solution after about 10 iterations. In Figure 11-b), the classical NSGA-II fell into a local optimum and failed to find the optimal solution. INSGA-II jumped out of the local optimum multiple times. Therefore, INSGA-II had a fast convergence speed and

strong optimization performance, demonstrating good

scheduling performance.

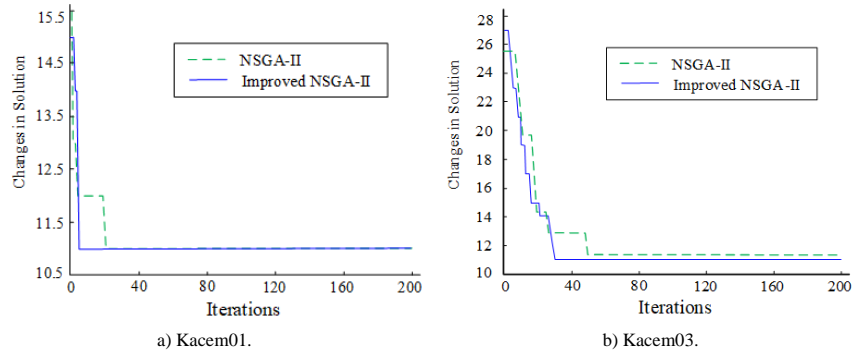


Figure 11. Comparison of search processes for solving kacem01 and kacem03 problems.

In Table 2, the test results of INSGA-II, classical NSGA-II, Improved Genetic Algorithm (IGA) combined with reactivation mechanism, Powell Search Method Genetic Algorithm (PSM-GA) and Multi-Objective Genetic Algorithm (MOGA) on the

Brandomarte case were compared. Among the six test cases, INSGA-II showed the best optimization performance, and obtained the shortest MCT. Therefore, INSGA-II had certain feasibility and effectiveness.

Table 2. Brandomarte case test results.

Example	Optimal solution	Algorithms				
		NSGA-II	IGA	PSM-GA	MOGA	INSGA-II
MK01	[36, 42]	40	40	40	40	40
MK02	[24, 32]	29	28	26	28	26
MK03	[204, 211]	208	204	204	206	204
MK04	[48, 81]	68	65	61	66	60
MK05	[168, 186]	180	176	173	178	173
MK06	[33, 86]	-	-	65	68	59

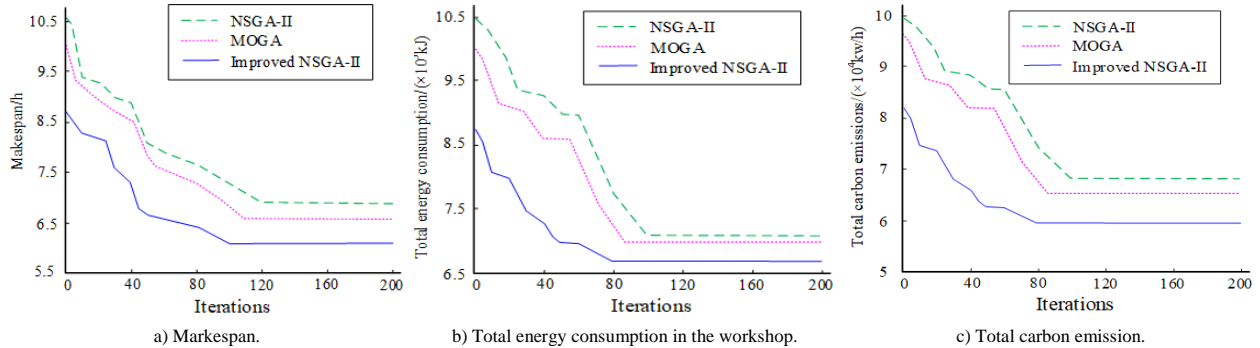


Figure 12. Iterative curve comparison.

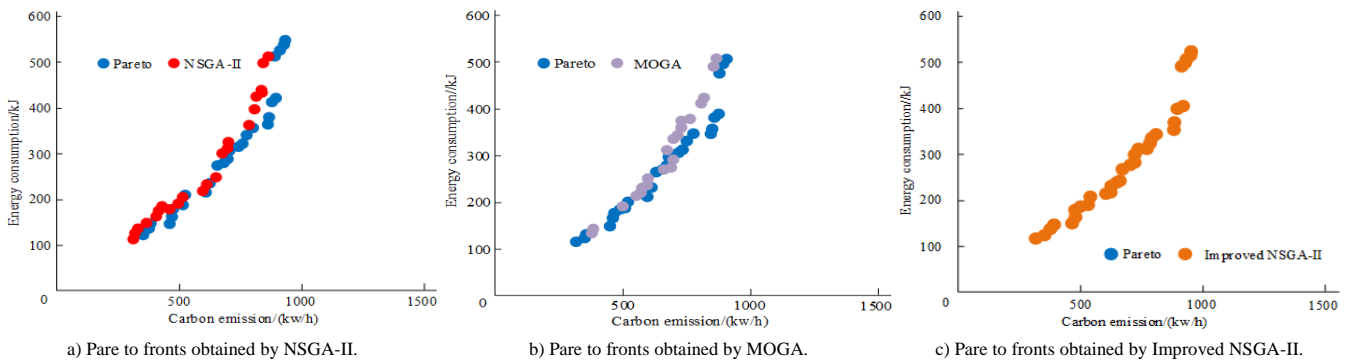


Figure 13. Pareto frontier comparison.

In Figure 12, this study took a manufacturing workshop as an example and used classical NSGA-II, MOGA, and INSGA-II algorithms in MATLAB software to optimize and solved the three objectives in the MI-LSCW model. In Figure 12-a), INSGA-II

performed the best in minimizing the MCT, with the lowest MCT of 6.12 hours. The MCT for MOGA and classical NSGA-II was both over 6.5 hours. In Figure 12-b), the total ES calculated by INSGA-II was the lowest, at 6.71×10^5 kJ. In Figure 12-c), the CE obtained

by INSGA-II was still the lowest, at 5.92×10^4 kw/h. Therefore, INSGA-II performed well in solving the MI-LSCW model, and could solve scheduling schemes with shorter completion time, less total ES, and CE, which had certain feasibility and effectiveness.

In Figure 13, the Pareto front gotten by INSGA-II was compared with classical NSGA-II and MOGA. INSGA-II had better approximation and distribution, and had stronger performance in solving MI-LSCW models.

5. Conclusions

To reduce CE in the manufacturing workshop while ensuring production efficiency, this study constructs an MI-LSCW model with three optimization objectives: minimizing MCT, minimizing total ES, and minimizing CE. An INSGA-II is constructed. As the number of targets increased, the IGD and SM values of the four algorithms gradually increased. When solving DTLZ1, the IGD value of INSGA-II was always the lowest, and when the number of targets was 20, the IGD value was 0.338. INSGA-II performed the best in the SM metric, with an SM value of 0.013 when the target quantity was 20. In the solution of DTLZ2, when the number of targets was 20, the IGD value of INSGA-II was 1.153 and the SM value was 0.415. INSGA-II performed the best in solving DTLZ1 and DTLZ2, with the lowest IGD and SM values. The IGD and SM values of classical NSGA-II were the highest. In the solution of Kacem01, both INSGA-II and classical NSGA-II could solve for the optimal solution, but INSGA-II had a faster solving speed and converged to the optimal solution in about 10 iterations. The MCT solved by INSGA-II was the shortest, which was 6.12 hours. The MCT for MOGA and classical NSGA-II was both over 6.5 hours. The total ES and CE calculated by INSGA-II were the lowest, with values of 6.71×10^5 kJ and 5.92×10^4 kw/h. INSGA-II had better approximation and distribution, and had stronger performance in solving MI-LSCW models. Thus, the INSGA-II had good convergence performance and has also demonstrated good results in solving LSCW problems. The proposed low-carbon scheduling model and INSGA-II algorithm have broad application potential in MO collaborative optimization in multiple practical, complex industrial scenarios, such as automobile manufacturing, electronic precision manufacturing, and processing large components in the aerospace industry. It can optimize workpiece sequence and equipment allocation, reduce high-ES equipment idle and material handling CEs. However, to simplify calculations, current research models primarily focus on static scheduling environments. These models assume that machines will not experience unexpected stops during the production process. The actual workshop often faces dynamic disturbances, such as machine failures, emergency order insertion, or raw material shortages. Therefore, in future research, further analysis

should be conducted on unexpected situations such as machine failures and emergency order insertion. To build a workshop low-carbon scheduling model that is more in line with actual production situations, the proposed algorithm should be embedded into an event-driven rescheduling framework to cope with dynamic disturbances or integrated with real-time workshop IoT data for online optimization and evaluation.

Funding

This article is a research result of the 2025 Jiaxing Municipal Public Welfare Research Program project, "Research on Intelligent Operation and Maintenance Large Model Technology of Compressor Production Process" (2025CGZ046). Key technologies and applications for process monitoring and situational analysis of industrial systems (2024SZD0220).

References

- [1] Chen C., Wu X., Ma J., Chen Y., and et al., "Optimal Low-Carbon Scheduling of Integrated Local Energy System Considering Oxygen-Enriched Combustion Plant and Generalized Energy Storages," *IET Renewable Power Generation*, vol. 16, pp. 671-687, 2022. <https://doi.org/10.1049/rpg2.12342>
- [2] Doerr B. and Qu Z., "A First Runtime Analysis of the NSGA-II on a Multimodal Problem," *IEEE Transactions on Evolutionary Computation*, vol. 27, pp. 1288-1297, 2023. <https://doi.org/10.1109/TEVC.2023.3250552>
- [3] Feng H., Zheng L., and Qiao S., "General Layout Planning Model of Landscape Ceramic Sculpture based on NSGA-II Algorithm," *Scalable Computing: Practice and Experience*, vol. 24, no. 3, pp. 371-378, 2023. <https://doi.org/10.12694/scpe.v24i3.2273>
- [4] Haghgoei A., Irajpour A., and Hamidi N., "A Multi-Objective Optimization Model of Truck Scheduling Problem using Cross-Dock in Supply Chain Management: NSGA-II and NRGA," *Journal of Modelling in Management*, vol. 19, pp. 1155-1179, 2024. <https://doi.org/10.1108/JM2-06-2023-0130>
- [5] Kabiri N., Emami S., and Safaei A., "Simulation-Optimization Approach for the Multi-Objective Production and Distribution Planning Problem in the Supply Chain: Using NSGA-II and Monte Carlo Simulation," *Soft Computing*, vol. 26, pp. 8661-8687, 2022. <https://doi.org/10.1007/s00500-022-07152-2>
- [6] Khettabi I., Benyoucef L., and Boutiche M., "Sustainable Multi-Objective Process Planning in Reconfigurable Manufacturing Environment: Adapted New Dynamic NSGA-II vs New NSGA-III," *International Journal of Production Research*,

vol. 60, pp. 6329-6349, 2022. <https://doi.org/10.1080/00207543.2022.2044537>

[7] Li H., Xu G., Wang D., Zhou M., and et al., "Chaotic-Nondominated-Sorting Owl Search Algorithm for Energy-Aware Multi-Workflow Scheduling in Hybrid Clouds," *IEEE Transactions on Sustainable Computing*, vol. 7, pp. 595-608, 2022. <https://doi.org/10.1109/TSUSC.2022.3144357>

[8] Li Z., Sang H., Pan Q., Gao K., and et al., "Dynamic AGV Scheduling Model with Special Cases in Matrix Production Workshop," *IEEE Transactions on Industrial Informatics*, vol. 19, pp. 7762-7770, 2023. <https://doi.org/10.1109/TII.2022.3211507>

[9] Liu C., Xin L., and Li J., "Environmental Regulation and Manufacturing Carbon Emissions in China: A New Perspective on Local Government Competition," *Environmental Science and Pollution Research*, vol. 29, pp. 36351-36375, 2022. <https://doi.org/10.1007/s11356-021-18041-w>

[10] Liu D., "Convergence of Energy Carbon Emission Efficiency: Evidence from Manufacturing Sub-Sectors in China," *Environmental Science and Pollution Research*, vol. 29, pp. 31133-31147, 2022. <https://doi.org/10.1007/s11356-022-18503-9>

[11] Ma H., Zhang Y., Sun S., Liu T., and Shan Y., "A Comprehensive Survey on NSGA-II for Multi-Objective Optimization and Applications," *Artificial Intelligence Review*, vol. 56, pp. 15217-15270, 2023. <https://doi.org/10.1007/s10462-023-10526-z>

[12] Ma S., Zhang A., Gu J., Qi Y., and et al., "Multi-Objective Optimization of Process Parameters for Ultra-Narrow Gap Welding Based On Universal Kriging and NSGA-II," *China Welding*, vol. 32, pp. 28-35, 2023. <https://dx.doi.org/10.12073/j.cw.20230121001>

[13] Maroua G., Leyla B., Laid K., and Saber B., "An Efficient Parallel Version of Dynamic Multi-Objective Evolutionary Algorithm," *The International Arab Journal of Information Technology*, vol. 19, no. 3A, pp. 422-431, 2022. <https://www.iajat.org/portal/images/Year2022/No.3A/22029.pdf>

[14] Mou J., Gao K., Duan P., Li J., and et al., "A Machine Learning Approach for Energy-Efficient Intelligent Transportation Scheduling Problem in a Real-World Dynamic Circumstances," *IEEE Transactions on Intelligent Transportation Systems*, vol. 24, pp. 15527-15539, 2022. <https://doi.org/10.1109/TITS.2022.3183215>

[15] Ning T. and Huang Y., "Low Carbon Emission Management for Flexible Job Shop Scheduling: A Study Case in China," *Journal of Ambient Intelligence and Humanized Computing*, vol. 14, pp. 789-805, 2023. <https://doi.org/10.1007/s12652-021-03330-6>

[16] Qiu M., Zhang J., Wang H., Yang C., and et al., "Multi-Objective Optimization Design of Wheel Hub Bearings Based on Kriging-NSGA-II," *Journal of Mechanical Science and Technology*, vol. 38, pp. 1341-1353, 2024. <https://doi.org/10.1007/s12206-024-0129-6>

[17] Shao W., Shao Z., and Pi D., "A Multi-Neighborhood-based Multi-Objective Memetic Algorithm for the Energy-Efficient Distributed Flexible Flow Shop Scheduling Problem," *Neural Computing and Applications*, vol. 34, pp. 22303-22330, 2022. <https://doi.org/10.1007/s00521-022-07714-3>

[18] Shoaei M. and Samouei P., "Clusters of floor Locations-Allocation of Stores to Cross-Docking Warehouse Considering Satisfaction and Space Using MOGWO and NSGA-II Algorithms," *Flexible Services and Manufacturing Journal*, vol. 36, pp. 315-342, 2024. <https://doi.org/10.1007/s10696-023-09489-8>

[19] Shu Z., Song A., Wu G., and Pedrycz W., "Variable Reduction Strategy Integrated Variable Neighborhood Search and NSGA-II Hybrid Algorithm for Emergency Material Scheduling," *Complex System Modeling and Simulation*, vol. 3, pp. 83-101, 2023. <https://doi.org/10.23919/CSMS.2023.0006>

[20] Tang Q., Ma L., Zhao D., Sun Y., and Wang Q., "A Dual-Robot Cooperative Arc Welding Path Planning Algorithm based on Multi-Objective Optimization," *IFAC-PapersonLine*, vol. 56, no. 2, pp. 3048-3053, 2023. <https://doi.org/10.1016/j.ifacol.2023.10.1433>

[21] Tian Y., Si L., Zhang X., Tan KC., and Jin Y., "Local Model-based Pareto Front Estimation for Multiobjective Optimization," *IEEE Transactions on Systems, Man, and Cybernetics: Systems*, vol. 53, pp. 623-634, 2022. <https://doi.org/10.1109/TSMC.2022.3186546>

[22] Tliba K., Diallo T., Penas O., Ben Khalifa R., and et al., "Digital Twin-Driven Dynamic Scheduling of a Hybrid Flow Shop," *Journal of Intelligent Manufacturing*, vol. 34, pp. 2281-2306, 2023. <https://doi.org/10.1007/s10845-022-01922-3>

[23] Trivedi M. and Sharma K., "Construction Time-Cost-Resources-Quality Trade-off Optimization Using NSGA-III," *Asian Journal of Civil Engineering*, vol. 24, pp. 3543-3555, 2023. <https://doi.org/10.1007/s42107-023-00731-0>

[24] Xu E., Li Y., Liu Y., Du J., and Gao X., "Energy Saving Scheduling Strategy for Job Shop Under TOU and Tiered Electricity Price," *Alexandria Engineering Journal*, vol. 61, pp. 459-467, 2022. <https://doi.org/10.1016/j.aej.2021.06.008>

[25] Yan N., Ma G., Li X., and Guerrero J., "Low-Carbon Economic Dispatch Method for Integrated

Energy System Considering Seasonal Carbon Flow Dynamic Balance," *IEEE Transactions on Sustainable Energy*, vol. 14, pp. 576-586, 2022. <https://doi.org/10.1109/TSTE.2022.3220797>

[26] Yang B., Pang Z., Wang S., Mo F., and Gao Y., "A Coupling Optimization Method of Production Scheduling and Computation Offloading for Intelligent Workshops with Cloud-Edge-Terminal Architecture," *Journal of Manufacturing Systems*, vol. 65, pp. 421-438, 2022. <https://doi.org/10.1016/j.jmsy.2022.10.002>

[27] Zhang F., "Constructing a Multi-Objective Optimization Model for Engineering Projects Based on NSGA-II Algorithm Under the Background of Green Construction," *Decision Making: Applications in Management and Engineering*, vol. 7, pp. 37-53, 2024. <https://doi.org/10.31181/dmame712024895>

[28] Zhang S., Zhou Z., Luo R., Zhao R., and et al., "A Low-Carbon, Fixed-Tour Scheduling Problem with Time Windows in a Time-Dependent Traffic Environment," *International Journal of Production Research*, vol. 61, pp. 6177-6196, 2023. <https://doi.org/10.1080/00207543.2022.2153940>

[29] Zhang Z., Yan J., Lu X., Zhang T., and Wang H., "Optimization of Porosity and Surface Roughness of CMT-P Wire Arc Additive Manufacturing of AA2024 Using Response Surface Methodology and NSGA-II," *Journal of Materials Research and Technology*, vol. 24, pp. 6923-6941, 2023. <https://doi.org/10.1016/j.jmrt.2023.04.259>

[30] Zhong Z., Jiang H., and Zuo H., "An Optimization Method of Electrostatic Sensor Array Based on Kriging Surrogate Model and Improved Non-Dominated Sorting Genetic Algorithm with Elite Strategy Algorithm," *Journal of Aerospace Engineering*, vol. 238, pp. 198-210, 2024. <https://doi.org/10.1177/09544100231219945>

[31] Zhuo W., Tan G., Chen Q., Hou Z., and et al., "Multi-Objective Optimization of Resistance Spot Welding Process Parameters of Ultra-High Strength Steel Based on Agent Model and NSGA-II," *Transactions of the China Welding Institution*, vol. 45, pp. 20-25, 2024. <https://dx.doi.org/10.12073/j.hjxb.20230317002>



Yanjun Zhou obtained her Master's degree in Electronic and Communication Engineering from Zhejiang University in 2011. In recent years, she has focused on research in Electrical Automation. Presently, she is an Associate Professor in Electrical Automation Technology at Jiaxing Nanyang Polytechnic Institute. Her research areas include Industrial Control, Digital Twins, and Intelligent Operation and Maintenance of Industrial Processes. She has conducted numerous training sessions and provided technical guidance to Enterprises on Industrial Robot Programming, Modern Industrial Control, and Production Management. She has published articles in more than 10 domestic and international journals.



Fei Wang is currently a Doctoral Candidate at College of Control Science and Engineering, China University of Petroleum (East China), China. His research interests include Intelligent Manufacturing, Human-Machine System, Industrial Internet, Artificial Intelligence and Digital twin.